# Female patient-specific finite element modeling of pelvic organ prolapse (POP)

Zhuowei Chen, Pierre Joli, Zhi-Qiang Feng, Mehdi Rahim, Nicolas Pirró,, Marc-Emmanuel Bellemare

# Female patient-specific finite element modeling of pelvic organ prolapse (POP)

Z.-W. Chen [a], P. Joli [a], Z.-Q. Feng [a,b,*], M. Rahim [c], N. Pirró [d], M. E. Bellemare [c]

[a] *Laboratoire de Mécanique et d'Energétique d'Évry, Université d'Évry-Val d'Essonne, Évry, France*

[b] *School of Mechanics and Engineering, Southwest Jiaotong University, Chengdu, China*

[c] *Laboratoire des Sciences de l'Information et des Systèmes, Marseille, France*

[d] *Service de Chirurgie Digestive, Hôpital la Timone, Marseille, France*

**Abstract**

Pelvic organ prolapse (POP) occurs only in women and becomes more common as women age. However, the surgical practices remain poorly evaluated. The realization of a simulator of the dynamic behavior of the pelvic organs is then identified as a need. It allows the surgeon to estimate the functional impact of his actions before his implementation. In this work, the simulation will be based on a patient-specific approach in which each geometrical model will be carried out starting from magnetic resonance image (MRI) acquisition of pelvic organs of one patient. To determine the strain and stress in the biological soft tissues, hyperelastic constitutive laws are used in the context of finite element analysis. The Yeoh model has been implemented into an in-house finite element code FER to model these organ tissues taking into account large deformations with multiple contacts. A 2D model is considered in this

preliminary study and the results show that our method can help to improve the understanding of different forms of POP.

*Key words:* Pelvic organ prolapse, Finite element method, Soft tissue, Hyperelasticity, Deformation

## 1 Introduction

Pelvic organ prolapse (POP) occurs only in women and becomes more common as women age. It refers to the loss of support to the structures contained within the bony pelvis and describes the descent of the pelvic organs into the vagina (Luft, 2006). By some estimates, about half of parous women experience some degree of prolapse and that 10-20% seeks medical care (Thakar & Stanton, 2002). POP repairs consist of 20% of the gynaecological surgeries (Jackson & Smith, 1997). Symptoms associated with POP are various degrees of pelvic pressure, low back pain, vulvovaginal excoriation, bowel dysfunction and sexual difficulties (Hagen, Stark, & Cattermole, 2004). Reported by US National Center for Health Statistics that in 2007, POP was a common diagnoses associated with hysterectomy, resulting in more than 517,000 surgical procedures (Hall, DeFrances, Williams, Golosinskiy, & Schwartzman, 2010). However, the surgical practices remain poorly evaluated. It has been estimated that the recurrence of POP in nearly one third of women after repair surgery (Olsen, Smith, Bergstrom, Colling, & Clark, 1997), and that 80% of these cases recur within two years of surgery (Baden & Walker, 1992). The use of precise

* Corresponding author. Tel.: +33 1 69 47 75 01; Fax: +33 1 69 47 75 99.

*E-mail address*: feng@ufrst.univ-evry.fr (Z.-Q. Feng)

numerical models of the female pelvic system will, in the future, provide the tools to simulate the dynamic behavior of pelvic organs. The realization of a simulator will allow surgeons to estimate the functional impact of his actions before implementation, to perform the surgery in a more controlled and reliable way.

In order to achieve these goals, we need to study the morphology and anatomy of these organs, to understand their environment and function to obtain meaningful boundary conditions and to determine material properties (Fung, 1993). From a mechanical point of view, the pelvic organs have specific geometries and material properties. They can be thought of as biomechanical structures which move and interact with each other due to external pressures, while the constraints are induced by rigid bodies (bones) as well as soft tissues such as muscles, ligaments and fascias, all ensuring the stability of these organs.

In the modeling works of the consulted literatures, biological soft tissues are usually subjected to large deformations with negligible volume change and show a highly non-linear anisotropic mechanical response due to their internal structure (Pena, Martínez, Calvo, & Doblar, 2006). To determine the strain and stress in the biological soft tissues such as ligaments, tendons or arterial walls, Spencer (Spencer, 1954) firstly developed the framework of continuum mechanics by means of the definition of a strain energy density function expressed in terms of kinematic invariants to model the purely elastic response of these tissues. This approach was further adapted to finite element formulations of soft collagenous biological tissues (see for example (Weiss, Maker, & Govindjee, 1996; Pena, del Palomar, Calvo, Martínez, & Doblar, 2007) for ligaments and (Holzapfel, Gasser, & Ogden, 2000) for arteries). However, a large number of elements of living organisms show very distinct anisotropic mechanical

properties (Holzapfel, 2006). Most energy densities used to model transversely isotropic and orthotropic soft tissues take a power law form (Schröder, Neff, & Balzani, 2005) or present an exponential behavior (Fung, Fronek, & Patitucci, 1979; Holzapfel et al., 2000). Although there might be some distinctions between quadrupedal and bipedal, the mechanical anisotropy properties of ewe vaginal tissue was highlighted in the tests of Rubod et al. (Rubod, Boukerrou, Brieu, Dubois, & Cosson, 2006a). Uniaxial tension tests were performed on the samples of vaginal tissue of patients with POP and fresh cadavers without prolapse (nPOP) (Jean-Charles et al., 2010), it shows that POP is significantly stiffer than nPOP tissue, both on anterior and posterior walls. Biomechanical properties of the vagina, aponeurosis and skin were compared (Gabriel et al., 2011), it turns out that the aponeurosis was much more rigid and less extendible than the vagina and skin, vaginal tissue was less rigid but more extendible than skin. In our work, Yeoh is chosen to model the isotropic and hyperelastic behavior of pelvic organs, and different material parameters are considered for different parts of the pelvic system.

Numerical simulations of interactions between male pelvic organs (bladder, prostate and rectum) and modeling approaches of female POP have already been performed (Boubaker, Haboussi, Ganghoffer, & Aletti, 2009; Venugopala Rao, Rubod, Brieu, Bhatnagar, & Cosson, 2010). Since intra-abdominal pressure has been considered as the cause of some multi-organ dysfunction (Cobb et al., 2005; Chionh, Wei, Martin, & Opdam, 2006), a 2.5 MPa pressure is applied on the surface of pelvic organ models by Venugopala Rao et al. (Venugopala Rao et al., 2010) while in the work of Boubaker et al. (Boubaker et al., 2009), only internal pressures are applied on the internal surfaces of bladder and rectum. A 'bear down' simulation of pelvic floor muscles was performed by Noakes

et al. (Noakes, Pullan, Bissett, & Cheng, 2008). In their work, an average downwards displacement of 27.2 mm and an average posterior displacement of 18.4 mm were produced due to a pressure of 4 kPa applied on the levator ani. It's very cumbersome to estimate the exact load on the pelvic system, so in present work, a displacement of 27.9 mm is identified and applied on the digitized surface of the pelvic floor muscle in the dynamic magnetic resonance image (MRI) sequence (Noakes et al., 2008).

The purpose of this study is to present preliminary 2D simulation results of interactions between pelvic organs during prolapse process using the finite element method on computational meshes based on live subject data. The paper is organized as follows: in Section 2, the establishment of a geometrical model is introduced based on the MRI of a specific patient. In Section 3, the anatomic description of the pelvic system is introduced. The structural and mechanical properties of the organ tissues are presented. In Section 4, the material parameters of the postulated constitutive laws are identified from literatures and the boundary conditions are established. Two simulation results are presented and discussed afterwards. In the last section, the conclusion and some perspectives of this project are proposed.

## 2 Geometrical definition of pelvic organs

To determine a realistic behavior of the organs, an accurate geometric model associated with a physical modeling is required. The geometric modeling of pelvic organs consists of medical imaging to reconstruct 3D models on which we must implement physical models and a numerical solution based on a spatial discretization from the finite element method. A geometrical rebuilding

of the pelvic organs of a female patient with no history of pelvic pathology perineal is performed with MRI data (Pirró et al., 2009). The acquisition of T2 static sagittal images of pelvic organs, with a thickness of 1 mm, was obtained in the supine position using a surface antenna (TR = 5.5 ms, TE = 2.7 ms, 256 × 256 matrix) (Fig. 1). This acquisition was the basis of pelvic model. A sagittal dynamic acquisition of thick sections of 10 mm was also performed at rest and during thrust using a dynamic turbo T2 sequence (TR = 3.6 ms, TE = 1.8 ms, FOV = 24 cm, 256 × 256 matrix).

The three-dimensional solid model was obtained from static images of MRI using free software segmentation (ITK-SNAP) based on the evolution of an active contour. The software can visualize simultaneously the organs in three planes and define the boundaries of areas to be segmented. A volumetric germ was placed in the defined area (Fig. 2), it grew automatically until it reached the defined limits. The cease of segmentation was automatic and was based on the variation of volume of the volumetric germ. At the end of the segmentation process, the geometrical irregularities were automatically corrected by smoothing, the three dimensional geometric model was generated as shown in Fig. 3. A thickness is added with an offset formulation, and the geometric model is finally exported in a hexahedral mesh (Bay et al., 2012). As a preliminary study of pelvic organs, a 2D model obtained in the sagittal plane is considered to test the capability of the developed algorithms and software to deal with large deformation hyperelastic problems with contact interfaces.

## 3 Characterization of pelvic organs

To perform a numerical simulation of the pelvic organ's motion and deformation, it is essential to have a good recognition of the environment and location of the pelvic organs and to determine their material properties.

### *3.1 From an anatomical point of view*

To have a good geometrical description of the true pelvis also called pelvic cavity leads us to the recognition of the anatomy of the pelvic organs (bladder, uterus and rectum). Fig. 4 illustrates a normal female pelvic anatomy. The pelvic floor lies at the bottom of the abdominal cavity, with this position, it acts as a supportive layer that prevents the pelvic organs from falling down (DeLancey, 1993; Messelink et al., 2005). Bladder and rectum are positioned anteriorly and posteriorly in the pelvic cavity. The bladder is supported by the adjacent parts of the skeleton and the pelvic floor (Drake, Vogl, & Mitchell, 2010). The urethra passes through the pelvic floor to reach the perineum, where it opens outside. Following the sigmoid colon at the vertebra, the rectum ends in the anal canal, which crosses the pelvic floor to open in the perineum. The pelvic cavity contains most of the reproductive tract of women. The vagina crosses the pelvic floor and is inserted into the uterus in the pelvic cavity which is placed between the rectum and bladder (Drake et al., 2010). The uterus is stabilized by the existence of transverse ligaments, anterior (pubocervical) and posterior (utero-sacral) formed by the pelvic fascia and connected to the pelvis walls. These ligaments would act primarily at the cervix leaving some rotational mobility of the uterus to adapt to the repletion of the bladder and

rectum.

According to the anatomical analysis, the existing ligaments in a pelvic system for fixation are difficult to precisely individualise on MRI, thus we have these following biomechanical considerations for the mobility of organs:

- The outlet orifices of the urethra and vagina in the perineum are almost fixed points relative to pubic bone (except serious malfunction of the perineum).
- The musculoskeletal pelvis wall can be considered as fixed and rigid with respect to the elasticity of the pelvic organs.
- The rectum is attached to the pelvic floor. The dorsal part of the rectum almost does not move, it relies on the back of the pelvic floor.
- The bladder is attached to a part of the fascia stretched along a plane of inclination at the point of connection of two ureters and the urethra, acting like a hammock. It is slightly held at its apex in the direction of the umbilicus. It is also surrounded by lateral ligaments belonging to the fascia, which start from the pubis to rejoin the cervix.
- The uterus is supported at the cervix by a set of ligaments from the fascia. The vagina is maintained by the fascia more or less rigidly following the stiffness of this part of the fascia. The vagina is kept separate from the rectum through the septum.

### *3.2 Mechanical properties and constitutive laws*

To perform the numerical simulation, it is essential to characterize the mechanical behavior of pelvic tissues. Many uniaxial tension tests of pelvic tissues were performed and stress-strain curves were obtained (Rubod, Boukerrou, Brieu,

Dubois, & Cosson, 2006b; Gabriel et al., 2011) and a hyperelastic behavior of the tissues was highlighted. To determine the strain and stress in the biological soft tissues such as ligaments, tendons, pelvic organs or arterial walls, hyperelastic constitutive laws are often used in the context of finite element analysis. Many attempts have been made to develop a theoretical stress-strain relation that fits experimental results for hyperelastic materials (Charlton & Yang, 1994; Boyce & Arruda, 2000; Miehe, Göktepe, & Lulei, 2004).

In order to describe the geometrical transformation problems, the deformation gradient tensor is defined by

$$\mathbf{F} = \mathbf{I} + \nabla \mathbf{u}, \quad J = \det(\mathbf{F}) > 0 \tag{1}$$

where $\mathbf{I}$ is the unity tensor and $\mathbf{u}$ the displacement vector. Because of large displacements and rotations, Green-Lagrangian strain is adopted for the non-linear relationships between strains and displacements. We note $\mathbf{C}$ the stretch tensor or the right Cauchy-Green deformation tensor ($\mathbf{C} = \mathbf{F}^T\mathbf{F}$). The Green-Lagrangian strain tensor $\mathbf{E}$ is defined by

$$\mathbf{E} = (\mathbf{C} - \mathrm{I})/2 \tag{2}$$

In the case of hyperelastic law, there exists an elastic potential function $W$ (or strain energy density function) which is a scale function of one of the strain tensors, whose derivative with respect to a strain component determines the corresponding stress component. This can be expressed by

$$\mathbf{S} = \frac{\partial W}{\partial \mathbf{E}} = 2\frac{\partial W}{\partial \mathbf{C}} \tag{3}$$

where $\mathbf{S}$ is the second Piola-Kirchoff stress tensor. In the particular case of isotropic hyperelasticity, Eq. (3) can be written by

$$\mathbf{S} = 2\left[I_3\frac{\partial W}{\partial I_3}\mathbf{C}^{-1} + \left(\frac{\partial W}{\partial I_1} + I_1\frac{\partial W}{\partial I_2}\right)\mathbf{I} - \frac{\partial W}{\partial I_2}\mathbf{C}\right] \tag{4}$$

where $I_i$ (i = 1,2,3) denote the invariants of the right Cauchy-Green deformation tensor $\mathbf{C}$ :

$$I_1 = tr(\mathbf{C})\ ;\ \ I_2 = (I_1^2 - tr(\mathbf{C}^2))/2\ ;\ \ I_3 = \det(\mathbf{C}) \tag{5}$$

Among the various energy density functions available in the literature (Mooney, 1940; Rivlin, 1948; Arruda & Boyce, 1993; Harth-Smith, 1996; Gent, 1996; Lambert-Diani & Rey, 1998; Feng, Vallée, Fortuné, & Peyraut, 2006), we have chosen the Yeoh constitutive law for the simulation of the isotropic soft tissues. This model leads to a mathematical function that fits well with the experimental data because it takes into account the global form of the experimental stress-strain curve. This model has been implemented into the in-house finite element code FER (Feng, 2008). The Yeoh strain energy density formulation is given by

$$W(I_1) = \sum_{i=1}^{3} C_{i0}(I_1 - 3)^i + \frac{K}{2}(J-1)^2 \tag{6}$$

where $C_{i0}$ are the material constants. $K$ is user-defined parameter which can be interpreted as the bulk modulus of the material. It is noted that if $J$ approaches to unity, the last term of Eq. (6) will approach to zero, which corresponds to an incompressible Yeoh material.

By deriving the energy density Eq. (6) with respect to the three invariants, then reporting the results in Eq. (4) gives

$$\mathbf{S} = 2(\sum_{i=1}^{3} iC_{i0}(I_1 - 3)^{i-1})\mathbf{I} + K(J^2 - J)\mathbf{C}^{-1} \tag{7}$$

## 4 Finite element modeling

In order to test our algorithms on solving of hyperelastic problems with contact, we considered in our present work to simulate directly a 2D model in the sagittal plane. In this case, we start by selecting nodes belonging to a sagittal plane; then from these selected points, we create the contours in the plane using spline functions, which allows us to define the surfaces to be meshed.

This 2D model includes 3262 plane quadrilateral elements and 3430 nodes (Fig. 5). The organs were meshed as filled but with different materials zones shown with different colors as depicted in Fig. 5, in which orange represents the bladder, green represents the uterus and vagina, blue represents the rectum. The yellow area represents the nearly incompressible material which can be

assumed as liquid inside these organs, the effect of shear on the material surrounding is neglected. The facia connecting organs is represented by dark green area. The pubis is next to the bladder and is considered as fixed.

As introduced previously in Section 3, the pelvic organs have hyperelastic material properties. We decided to identify the coefficients of Yeoh model for each organ from the experimental results of Venugopala Rao et al. (Venugopala Rao et al., 2010), because the results are consistent with those of Boubaker's thesis (Boubaker, 2009), by using the identification function of MSC.Marc Mentat software. The material parameters for each organ from experimental data are obtained and presented in Table 1. The pubis is fixed without considering its deformation. To the authors' knowledge, there is no reference for the material inside the organs and the fascia, so we chose the parameters which make them more soft and incompressible than organs.

Two simulations of the 2D model are performed. The first is the prolapse of pelvic organs due to a single displacement, the second is a direct comparison with dynamic MRI images taken in the sagittal plane. The finite element simulation of interactions between pelvic organs is performed in the framework of large deformation, the total Lagrangian formulation is selected in this work to describe nonlinear behavior. A frictionless sliding contact with no interpenetration is considered between the deformable bodies (uterus and bladder) and between the bladder and pubis (Feng, Peyraut, & Labed, 2003; Feng, Peyraut, & He, 2006).

### *4.1 Simulation based on data from the literature*

It is difficult to estimate the exact load imposed on pelvic organs, therefore, for the first simulation, an inferior displacement of 27.9 mm which was identified on the digitized surface of the pelvic floor muscle in the dynamic MRI image sequence (Noakes et al., 2008) is applied on the upper anterior part of uterus to see the interactions and deformations of the pelvic system. The simulation was performed by the in-house solver FER and the results are displayed by the postprocessing software FER/View (Feng & Feng, 2004).

The boundary conditions are specified in terms of node displacements: the pubic bone is totally constrained ($U_x = U_y = 0$). As mentioned before, the pelvic floor lies at the bottom of these organs and acts as a supportive layer, although it was not defined in our model, but its effect was considered equally by fixing in one direction of the bottom of bladder, vagina and rectum, while allowing a little decline during POP ($U_x = 0$, $U_y = -10$ mm).

The simulation result is shown in Fig. 6. A comparison between initial configuration and deformed shape at last step is presented with the distribution of von Mises stress. We can see that the organ deformed as expected and the multi-contact between these organs was well handled. The maximum stress seems to occur in the anterior and posterior part of the vagina. It is well known that the anterior vaginal wall prolapse, clinically known as cystocele, is the most common form of pelvic organ prolapses (DeLancey, 1992). Among the women who had some form of prolapse, 34.3% have cystocele, 18.6% have rectocele and 14.2% have uterine prolapse (Hendrix et al., 2002). Both the cystocele and rectocele occur when the tissues and muscles that hold the or-

gans in place are stretched or weakened. They cause separately the bladder and rectum to move from its natural position and press against the forward and back wall of the vagina, as shown in the simulation result. Therefore, this model as well as our software could help understand the reasons of such form of prolapse and estimate the virtual effect of the organ's interactions.

### *4.2 Simulation based on dynamic MRI images*

The dynamic MRI acquisition, performed with a 1.5 T Philips *Gyroscan* in the sagittal plane, allows to observe the movements and deformations of pelvic organs. Each MRI sequence considered is a subset of 12 frames extracted from an acquisition during an abdominal pushing down maneuver. The 2D images of the MRI sequences are segmented in order to produce a set of closed contours of four organs of interest: bladder, rectum, uterus and vagina. Fig. 7 illustrates three frames of a MRI sequence, in which the first frame represents the organs at rest, the last frame shows the condition when the pushing down effort is at its maximum. From these contours, we can characterize the movement by calculating the center of mass of each organ, the organ trajectory will summarize the displacement (Rahim, Bellemare, Pirró, & Bulot, n.d.). We can also characterize the deformation by using the shape descriptors (Zhang & Lu, 2004). Two shapes of organs are compared by computing a distance between their own descriptor coefficients. The quantification process of the deformation will not be detailed in this paper, more informations can be found in (Rahim, Bellemare, Bulot, & Pirró, 2010). The displacement of contours between each frame is obtained, which has also been correlated with the nodes in the contours of our mesh model. By imposing the displacement on each

organ's contour, the contact forces can not be considered, which reveals the inter-penetration between organs. We have also removed the fascia part and the pubis to adapt the new condition. Fig. 8 shows the comparison between the simulation and dynamic MRI images of 12 frames.

## 5 Conclusion and perspectives

In this paper, we focused on the simulations of 2D model of pelvic organs. We have modeled one of the mechanical process occurring within the female pelvic organs in order to improve the understanding of POP. We have simulated the deformation of each organ by imposing the displacement calculated from a MRI sequence of 12 frames during an abdominal pushing down maneuver. The isotropic hyperelastic mechanical behavior is considered for the organ tissues. This is a first step which opens many perspectives and can propose a tool to help physicians to characterize functional impact of these organs. With this tool, it is possible to have a good idea of the contact force, the dimension of contact surface, the deepness of significant stresses, the energy absorbed by the soft tissue, etc.

Biological soft tissues are often assumed to be anisotropic and hyperelastic (Fung, 1993; Holzapfel et al., 2000). Therefore, as a perspective of this work, anisotropic material laws should be adopted in the future. Moreover, a three dimensional model based on MRI data including pelvic organs, pubic bone, as well as ligaments and fascias shall be used in further simulations. To improve the simulation accuracy, more realistic boundary conditions should be considered.

## Acknowledgement

This work is supported by the French ANR Grant (No. ANR-09-SYSC-008) and the National Natural Science Foundation of China (No. 11372260), which are greatly appreciated.

## References

Arruda, E. M., & Boyce, M. C. (1993). A three dimensional constitutive model for the large deformation stretch behavior of rubber elastic materials. *J. Mech. Phys. Solids*, *41*, 389-412.

Baden, W. F., & Walker, T. (1992). *Surgical repair of vaginal defects.* JB Lippincott.

Bay, T., Chen, Z.-W., Raffin, R., Daniel, M., Joli, P., Feng, Z.-Q., & Bellemare, M. (2012). Geometric modeling of pelvic organs with thickness. In *Ei2012-electronic imaging.* Burlingame, USA.

Boubaker, M. B. (2009). *Contribution mécanique à la rduction des marges en radiothérapie de la prostate: modélisation et simulation numérique du mouvement et de la déformation des organes pelviens* (Unpublished doctoral dissertation). Institut National Polytechnique de Lorraine, France.

Boubaker, M. B., Haboussi, M., Ganghoffer, J.-F., & Aletti, P. (2009). Finite element simulation of interactions between pelvic organs: Predictive model of the prostate motion in the context of radiotherapy. *J. Biomech.*, *42*, 1862-1868.

Boyce, M. C., & Arruda, E. M. (2000). Constitutive models of rubber elasticity: a review. *Rubber Chem. Technol.*, *73*, 504-523.

Charlton, D. J., & Yang, J. (1994). A review of methods to characterize rubber elastic behaviour for use in finite element analysis. *Rubber Chem. Technol.*, *67*, 481-503.

Chionh, J. J. L., Wei, B. . P. C., Martin, J. A., & Opdam, H. I. (2006). Determining normal values for intra-abdominal pressure. *ANZ J. Surg.*, *76*, 1106-1109.

Cobb, W. S., Burns, J. M., Kercher, K. W., Matthews, B. D., Norton, H. J., & Heniford, B. T. (2005). Normal intraabdominal pressure in healthy adults. *J. Surg. Res.*, *129*, 231-235.

DeLancey, J. O. (1992). Anatomic aspects of vaginal eversion after hysterectomy. *Am. J. Obstet. Gynecol*, *166*, 1717-24.

DeLancey, J. O. (1993). Anatomy and biomechanics of genital prolapse. *Clin. Obstet. Gynecol.*, *36*, 897-909.

Drake, R. L., Vogl, A. W., & Mitchell, A. W. M. (2010). *Gray's anatomie pour les étudiants(2e édition)*. Elsevier-Masson.

Feng, Z.-Q. (2008). *http://lmee.univ-evry.fr/∼feng/FerSystem.html.*

Feng, Z.-Q., & Feng, Z.-G. (2004). FER/View: An interactive finite element post-processor. In Z.-H. Yao, M.-W. Yuan, & W.-X. Zhong (Eds.), *Computational mechanics*. Beijing, China: Springer.

Feng, Z.-Q., Peyraut, F., & He, Q.-C. (2006). Finite deformations of Ogden's materials under impact loading. *Int. J. Non-linear Mech.*, *41*, 575-585.

Feng, Z.-Q., Peyraut, F., & Labed, N. (2003). Solution of large deformation contact problems with friction between Blatz-Ko hyperelastic bodies. *Int. J. Engng. Science*, *41*, 2213-2225.

Feng, Z.-Q., Vallée, C., Fortuné, D., & Peyraut, F. (2006). The 3é hyperelastic model applied to the modeling of 3D impact problems. *Finite Elem. Anal. Des.*, *43*, 51-58.

Fung, Y. C. (1993). *Biomechanics: Mechanical properties of living tissues.* Springer.

Fung, Y. C., Fronek, K., & Patitucci, P. (1979). Pseudoelasticity of arteries and the choice of its mathematical expression. *Am. J. Physiol.*, *237*, 620-631.

Gabriel, B., Rubod, C., Brieu, M., Dedet, B., Landsheere, L., Delmas, V., & Cosson, M. (2011). Vagina, abdominal skin, and aponeurosis: do they have similar biomechanical properties? *Int. Urogynecol. J.*, *21*, 23-27.

Gent, A. N. (1996). A new constitutive relation for rubber. *Rubber Chem. Technol.*, *69*, 59-61.

Hagen, S., Stark, D., & Cattermole, D. (2004). A united kingdom-wide survey of physiotherapy practice in the treatment of pelvic organ prolapse. *Physiotherapy*, *90*, 19-26.

Hall, M. J., DeFrances, C. J., Williams, S. N., Golosinskiy, A., & Schwartzman, A. (2010). National hospital discharge survey: 2007 summary. *National health statistics reports*, *29*, 1-24.

Harth-Smith, J. L. (1996). Elasticity parameters for finite deformations of rubber-like materials. *Math. Phys.*, *17*, 608-625.

Hendrix, S. L., Clark, A., Nygaard, I., Aragaki, A., Barnabei, V., & McTiernan, A. (2002). Pelvic organ prolapse in the women's health initiative: gravity and gravidity. *Am. J. Obstet. Gynecol*, *186*, 1160-1166.

Holzapfel, G. A. (2006). *Mechanics of biological tissue.* Springer.

Holzapfel, G. A., Gasser, T. C., & Ogden, R. (2000). A new constitutive framework for arterial wall mechanics and a comparative study of material models. *J. Elasticity*, *61*, 1-48.

Jackson, S., & Smith, P. (1997). Diagnosing and managing genitourinary prolapse. *Br. Med. J.*, *314*, 875-880.

Jean-Charles, C., Rubod, C., Brieu, M., Boukerrou, M., Fasel, J., & Cosson, M. (2010). Biomechanical properties of prolapsed or non-prolapsed vaginal tissue: impact on genital prolapse surgery. *Int. Urogynecol. J.*, *21*, 1535-1538.

Lambert-Diani, J., & Rey, C. (1998). New phenomenological laws for rubber and thermoplastic elastomers. *Eur. J. Mech.*, *1(18-6)*, 1027-1043.

Luft, J. (2006). Organ prolapse: current state of knowledge about this common condition. *J. Nurse Pract.*, *2(3)*, 170-177.

Messelink, B., Benson, T., Berghmans, B., Bø, K., Corcos, J., Fowler, C., ... Von Kerrebroeck, P. (2005). Standardization of terminology of pelvic floor muscle function and dysfunction: report from the pelvic floor clinical assessment group of the international continence society. *Neurourol. Urodynam.*, *24*, 374-380.

Miehe, C., Göktepe, S., & Lulei, F. (2004). A micro-macro approach to rubber-like materialspart i: The non-affine micro-sphere model of rubber elasticity. *J. Mech. Phys. Solids*, *52*, 2617-2660.

Mooney, M. (1940). A theory of large elastic deformation. *J. Appl. Phys.*, *11(9)*, 582-592.

Noakes, K. F., Pullan, A. J., Bissett, I. P., & Cheng, L. K. (2008). Subject specific finite elasticity simulations of the pelvic floor. *J. Biomech.*, *41*, 3060-3065.

Olsen, A. L., Smith, V. J., Bergstrom, J. O., Colling, J. C., & Clark, A. (1997). Epidemiology of surgically managed pelvic organ prolapse and urinary incontinence. *Obstet. Gynecol.*, *89*, 501-506.

Pena, E., del Palomar, A. P., Calvo, B., Martínez, M. A., & Doblar, M. (2007). Computational modelling of diarthrodial joints. physiological, pathological and post-surgery simulations. *Arch. Comput. Meth. Engrg*, *14(1)*,

1-54.

Pena, E., Martínez, M. A., Calvo, B., & Doblar, M. (2006). On the numerical treatment of initial strains in soft biological tissues. *Int. J. Numer. Meth. Engrg*, *68*, 836-860.

Pirró, N., Bellemare, M. E., Rahim, M., Durieux, O., Sielezneff, I., Sastre, B., & Champsaur, P. (2009). Résultats préliminaires et perspectives de la modélisation dynamique pelvienne patient-spécifique. *Pelv. Perineol.*, *4*, 15-21.

Rahim, M., Bellemare, M. E., Bulot, R., & Pirró, N. (2010). Pelvic organs dynamic feature analysis for MRI sequence discrimination. In *International conference on pattern recognition.* Istanbul.

Rahim, M., Bellemare, M. E., Pirró, N., & Bulot, R. (n.d.). A shape descriptors comparison for organs deformation characterization in MRI sequences..

Rivlin, R. S. (1948). Large elastic deformations of isotropic materials. IV. Further developments of the general theory. *Phil. Trans. R. Soc. Lond. A*, *241(835)*, 379-397.

Rubod, C., Boukerrou, M., Brieu, M., Dubois, P., & Cosson, M. (2006a). Biomechanical properties of vaginal tissue. part 1: New experimental protocol. *J. Urol.*, *178*, 320-325.

Rubod, C., Boukerrou, M., Brieu, M., Dubois, P., & Cosson, M. (2006b). Biomechanical properties of vaginal tissue. Part 1: New experimental protocol. *J. Urol.*, *178*, 320-325.

Schröder, J., Neff, P., & Balzani, D. (2005). A variational approach for materially stable anisotropic hyperelasticity. *Int. J. Solids. Struct.*, *42*, 4352-4371.

Spencer, A. J. M. (1954). Theory of invariants. *Continuum Physics, Academic Press, New York*, 239-253.

Thakar, R., & Stanton, S. (2002). Management of genital prolapse. *Br. Med. J.*, *324(7348)*, 1256-1262.

Venugopala Rao, G., Rubod, C., Brieu, M., Bhatnagar, N., & Cosson, M. (2010). Experiments and finite element modelling for the study of prolapse in the pelvic floor system. *Comput. Methods Biomech. Biomed. Eng.*, *13*, 349-357.

Weiss, J. A., Maker, B. N., & Govindjee, S. (1996). Finite element implementation of incompressible, transversely isotropic hyperelasticity. *Comput. Meth. Appl. Mech. Engng*, *135*, 107-128.

Zhang, D., & Lu, G. (2004). Review of shape representation and description techniques. *Pattern Recogn.*, *37*, 1-19.

Table 1

Material parameters of organs according to Yeoh strain energy density

| Material coefficients | Vagina(uterus) | Rectum | Bladder |
|---|---|---|---|
| $C_{10}$ (MPa) | 0.175 | 0.088 | 0.071 |
| $C_{20}$ (MPa) | 8.648 | 3.092 | 0.202 |
| $C_{30}$ (MPa) | 8.632 | 2.871 | 0.048 |
| $K$ (MPa) | 16.0 | 11.0 | 9.0 |

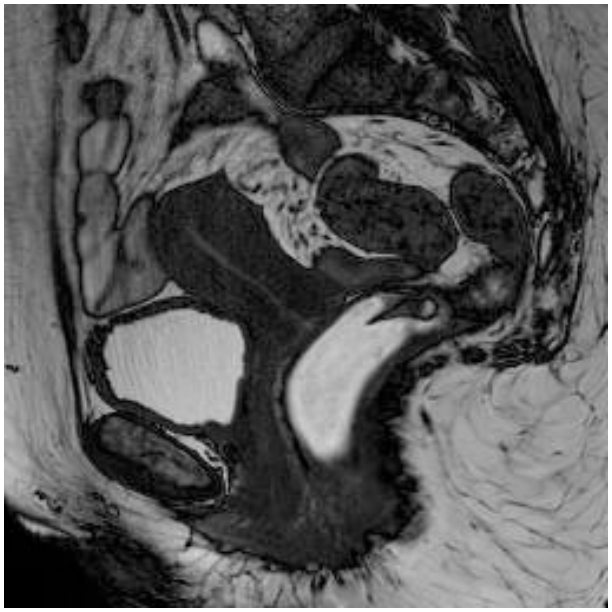

Fig. 1. MRI image for the development of the geometric model

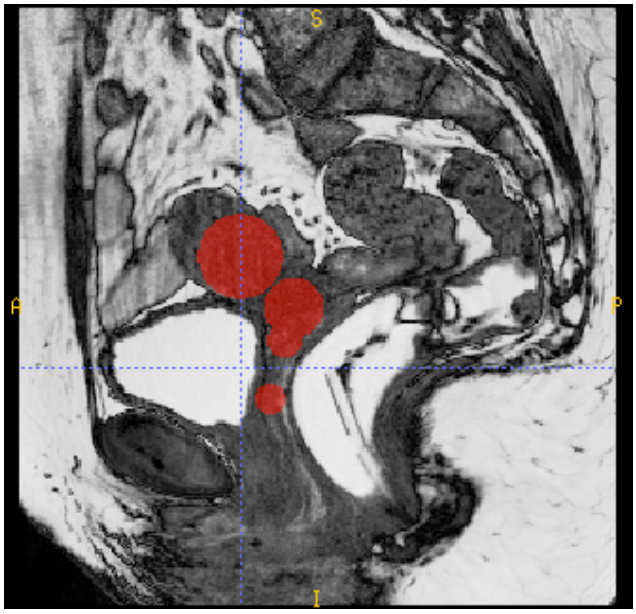


Fig. 2. Volumetric germs placed inside of the uterus and vagina

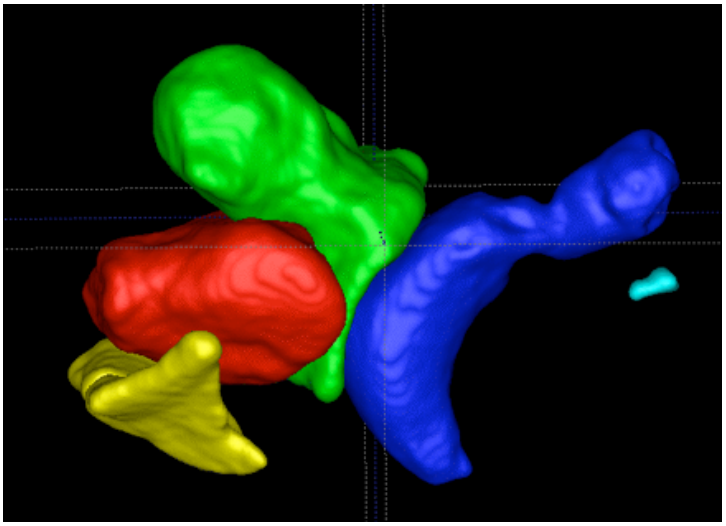

Fig. 3. Complete geometric model

Fig. 4. Schematic location of pelvic organs in the pelvic cavity

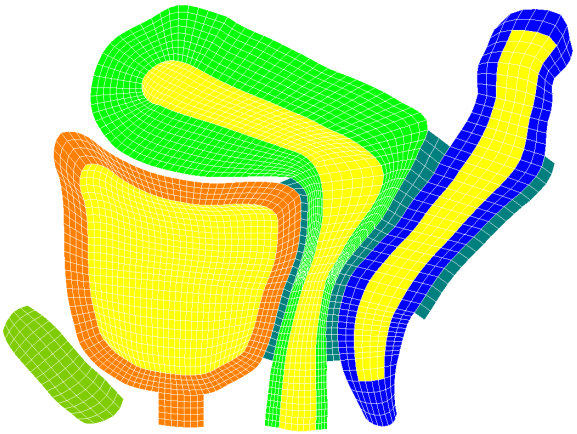

Fig. 5. Initial configuration and meshes

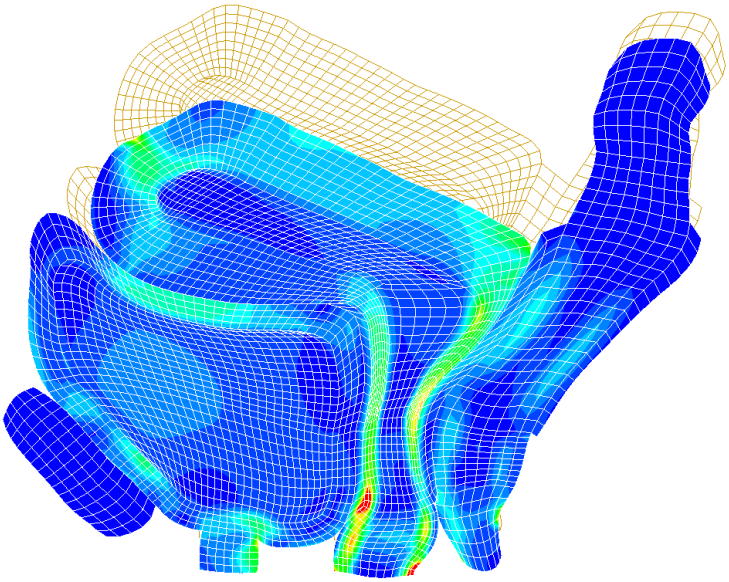

Fig. 6. Initial configuration and deformed shape with von Mises stress

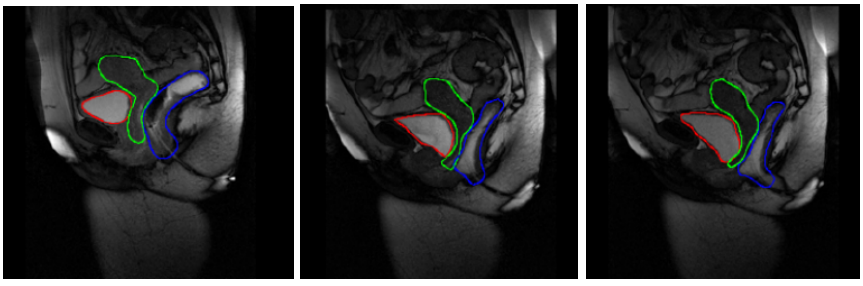

Fig. 7. Segmented MRI sequence

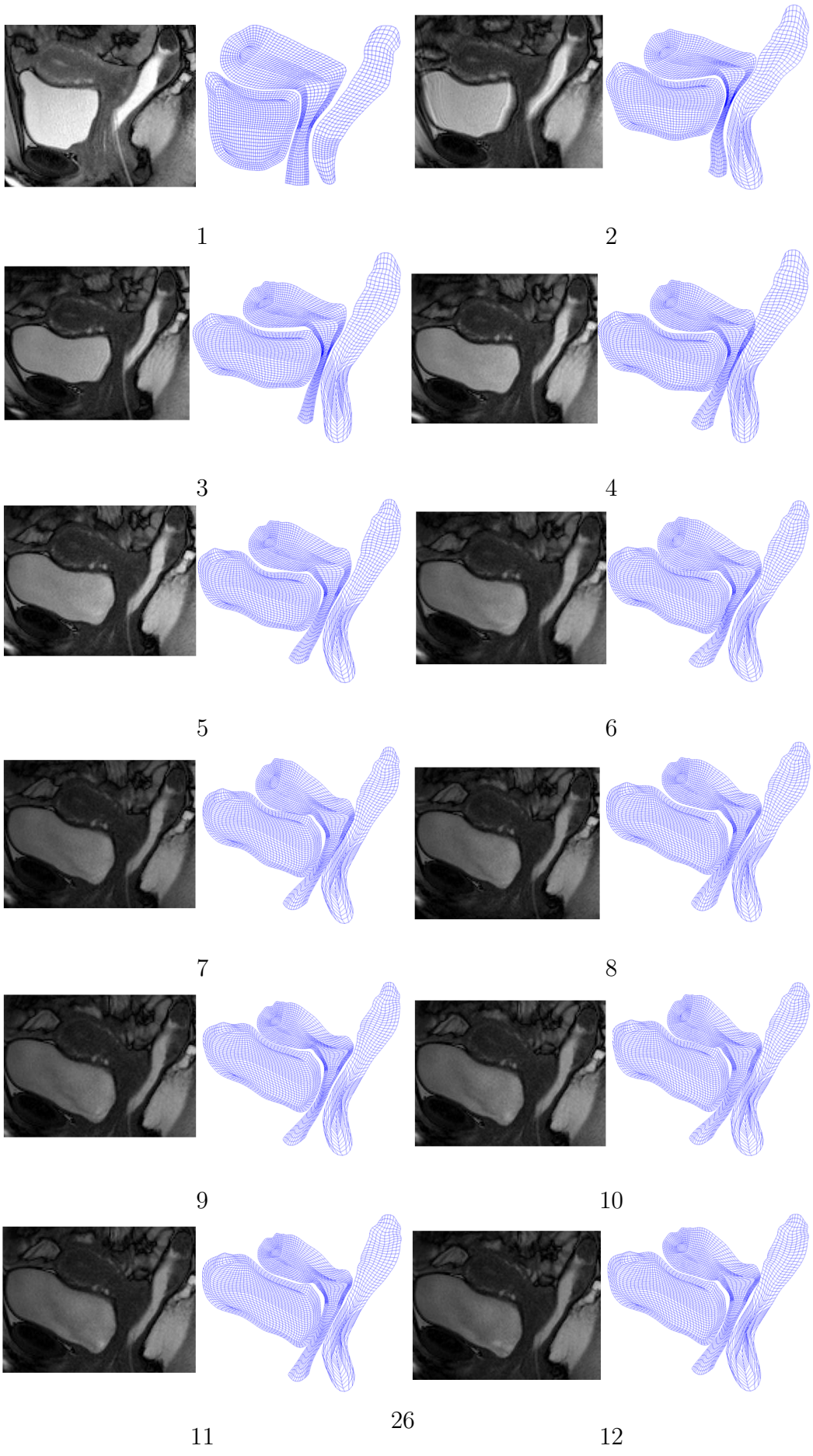


Fig. 8. Comparison of the deformation between numerical results and MRI images